1st International Conference on Experiments/Process/System Modelling/Simulation/Optimization
1st IC-EpsMsO
Athens, 6-9 July, 2005

RECENT ADVANCES ON FRICTION MODELLING WITHIN A COMPUTATIONAL MECHANICS FRAMEWORK

Achilles Vairis[1], Nicholas Christakis [2]

[1] Department of Mechanical Engineering
TEI of Crete
PO Box 1939, Heraklion 71004, Greece
E mail: vairis@stef.teiher.gr , web page: http://users.teicrete.gr/vairis

[2] Department of Applied Mathematics
University of Crete
Heraklion, 71409, Greece
E mail: nicholas.christakis@physics.org, web page: http://www.tem.uoc.gr.gr/~nchristakis

Keywords: friction coefficient, modelling, stick-slip

Abstract *Frictional forces both in microscopic and macroscopic scale affect the economics, operation and life of machines, both of the macro and nano scale type. Sliding frictional behaviour of an unlubricated similar metal couple was studied experimentally and was found to be strongly influenced by operating conditions such as sliding speed and interface temperature for the titanium alloy Ti6Al4V. The different friction regimes observed experimentally are explained using an analytical contact model. The analytical model represents the moving system of two interconnected plates at the sliding interface with bonds, which continuously form and rupture during sliding. Moreover, the characterised frictional behaviour, which depends on interface temperature, is used to model numerically the non-linear thermo-mechanical process of linear friction welding of Ti6Al4V.*

1. FRICTION STUDIES – PAST AND PRESENT

The movement of an object along a surface in the macro or nano scale is resisted by forces commonly referred to as friction. These forces are nonconservative and convert the kinetic energy of the moving objects into thermal or mechanical energy, as evident by the increase in temperature at the rubbing interface or squeaking noises. It is common experience that the necessary force to commence sliding a material is greater than that to maintain motion, and therefore the coefficient of static friction is greater than that of dynamic friction. It has also been observed that the range of values of frictional forces differ by orders of magnitude depending on the length scales of the applications, macroscopic or nanoscopic.
As the French physicist Guillaume Amonton [1] stated in his empirical law of sliding friction, the friction force is proportional to the normal load, or if expressed mathematically

$$\text{Friction force} = \text{coefficient of friction X normal load} \quad (1)$$

In most cases the precise value of the coefficient of friction depends strongly on the experimental conditions under which it is measured. In addition, a second law of friction states that friction force is independent of the apparent area of contact between the two surfaces. Charles Augustin de Coulomb, also, stated in his third law of macroscopic friction, that friction force is independent of sliding velocity. The coefficient of dynamic friction is expected to be nearly independent of ordinary sliding velocities, and similar behaviour is exhibited for temperature changes, unless phase transformations appear at the interface.
All three laws of friction, although not holding in every condition of stress, temperature, velocity and length scale, have far outlived a number of theoretical attempts to provide a clear explanation of the phenomenon as well as a unified theory for friction in both the macroscopic and the microscopic level. The difficulty in identifying the origin and method of development of friction at microscopic level lies with the enormous number of contacts which develop over time and are difficult to characterise.
Initial attempts, by Amontons and Coulomb among others, assumed that mechanical interlocking between rigid or elastically deforming asperities are responsible for the frictional force and the consequent mechanical wear and heat generation. This model assumes two bodies which perform both longitudinal and transverse motion at the same time; work is performed by normal load after the upper body has returned to its lowest position, and all of the potential energy is recovered. Unfortunately, macroscopic observations may not be in agreement with this theory as highly polished and smooth surfaces are necessary for cold welding and do not necessarily show low

friction. An additional problem for this theory, is that adsorbed films change friction by orders of magnitude while maintaining the same roughness of the surface.
A more successful model was proposed in the 1950s by Bowden and Tabor [2] which connected asperities and molecular adhesion. The actual area of contact is much smaller that the apparent area of contact by a factor of 10^4. Even so, surfaces do rest on each other on asperities which exhibit local yielding. When surfaces move relative to each other these bonds are damaged while new are formed, with friction being related to the shear strength of the material. Assuming that the normal pressure at the interface is independent of the normal load, then the friction coefficient can be estimated as

$$\text{Friction coefficient} = \text{shear strength} / \text{pressure} \quad (2)$$

Lacking precise and direct measurement methods for the true area of contact, contact mechanics models have been used. The most known model is one where contact between the two surfaces is represented by two spheres [3]. The true area of contact is proportional to the normal load to the power of n, where n is 2/3 for perfectly elastic deformation (as in the case of rubber, wood and textiles) and 1 for plastic deformation (as in the case of brittle materials like glass).
For multiple asperity contact [4] , which is closer to the physical situation, a linear relationship was found to be between the true area of contact and normal load for an exponential distribution of asperity heights, which also holds for a Gaussian distribution, and for fractal surface geometries. The significance of this linear relationship is that as the load increases the size of the individual contacts increases as well as the number of the contacts. This concept, which agrees with Bowden's model, does apply to a range of materials, but predicts a range of friction coefficient between 0.17 and 0.2, which is contradictory to experimental values. Wear rates and ploughing effects are not enough to explain this disparity.
Tomlinson [5] suggested that phononic or lattice vibration mechanisms could contribute to friction. When atoms near the interface are set to motion by atoms of the opposite rubbing interface, friction arises from phonons. Vibrations are produced when the mechanical energy necessary for sliding is converted to sound energy which in turn is converted to heat. The phononic approach was verified [6] as new experimental and theoretical techniques were available for investigating friction in the micro and nano scale. It has been observed that frequently static friction is absent and that solid-liquid and solid-solid interfaces follow a viscous-friction law.
In the macroscopic systems where everything is of different length and time scales, these fundamental energy dissipation mechanisms of phononic and electronic effects have not been clearly identified as yet, as Tabor had suspected. In addition, whereas the theoretical prediction that static friction disappears when clean surfaces deform elastically, in practice it does exist, is quite variable and is always larger than sliding friction.
A related phenomenon is stick-slip friction, where for certain sliding velocities the interface is repetitively sticking and slipping. This phenomenon is responsible for the screeching noises of car braking.
To relate the phenomena of static and stick slip friction further studies are necessary. As the interfacial geometry changes continuously, friction coefficients are affected and stick slip occurs. In addition, friction force at an individual asperity level can change with increasing load. These effects may be due to additional adsorbed molecules in the interface.
Unfortunately existing data and theoretical explanations are strongly depended on specific conditions, with linking between individual experimental results not fully established. Realistic laboratory experiments should be well controlled, provide a wealth of information and be relevant to operating machinery. It is estimated that developed countries can conserve up to 1.6 % of their GNP by limiting the negative effects of friction and wear, which cause entire mechanical systems to be routinely discarded after certain parts are worn, and by reducing consumed energy used in the manufacture of assemblies.

2. FRICTIONAL BEHAVIOUR EXPERIMENTS

Typical friction experiments involve pin and disk apparatus or some other mechanism where a pin slides over a given point on a surface intermittently. To successfully model manufacturing processes where friction plays an important role, such as friction welding, it is necessary to establish the friction characteristics of the materials involved under conditions that typify the system under study.
A number of measurements were made under different sliding conditions. Tubular specimens were used with typical dimensions of 22 mm length and radius r of 24 mm, and thin walls (1 mm) (see Fig.1). The experimental apparatus [7] was instrumented so that the interface coefficient of friction was measured indirectly. The stationary cylindrical specimen was placed in a fixture, which in turn rested on a Kistler piezoelectric transducer which measured directly the normal force exerted by the rotating specimen on the stationary specimen, and indirectly the horizontal friction force acting on the specimen. The vertical force applied on the specimen was transferred to the force measuring plate by means of a thrust bearing. The stationary specimen holder was free to rotate, resting on a thrust bearing that was firmly attached to the force transducer. As the bottom stationary specimen came in contact with the rotating specimen at the top, it would try to rotate as well only to be stopped by the pin. The horizontal reaction force L, which was produced by the friction force on the rotating interface, was

transmitted to the plate via a lever. Physically, the normal load N applied, the force L produced by the friction force and the friction coefficient μ can be related by

$$\mu = \frac{Ld / r}{N} \tag{3}$$

where d is the distance of the pin attached to the load cell plate from the centre of rotation, transmitting the friction force experienced by the stationary specimen, and r the radius of the cylindrical specimen.

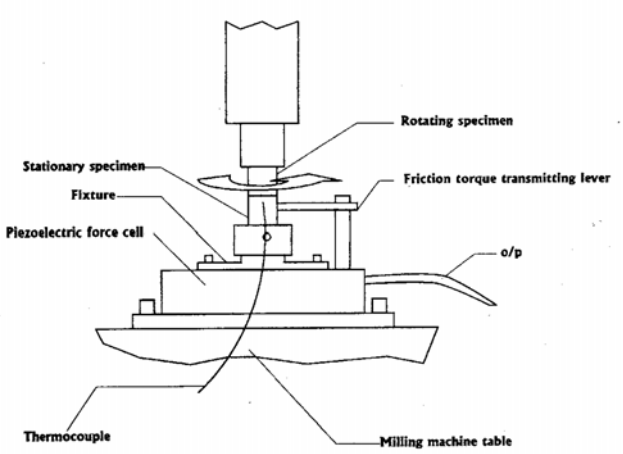

Figure 1. Frictional behaviour exeperiments apparatus

Alternatively, the coefficient of friction can be related to the stress conditions at the rubbing interface, with

$$\mu = \tau / \sigma \tag{4}$$

where τ is the shear stress at the rubbing interface, and σ is the normal stress at the rubbing interface.
Simultaneous measurements of N and L were used to determine the coefficient of friction μ experimentally. A thermocouple was used to record the temperature on the stationary specimen, which was spot welded on the outside face of the specimen at a known distance from the interface. The shortening of the specimens was also registered to compensate for the move of the rubbing interface closer to the thermocouple due to wear.
As the recorded temperature was an indirect measure of the actual rubbing interface temperatures, a non-linear finite element model was used to estimate the true temperatures encountered at the interface. Thermal loads were applied at one face of the block and the transient response to that load was calculated. The transient model incorporated the convective heat loss to the surroundings during the first few seconds after initial contact, from the side faces of the model, using a convection coefficient of 100 W/m^2/°C to represent the flow of air around the specimens, as well as conduction to the bulk of the block, which was initially at 20 °C. The numerical simulation enabled the prediction of the true interface temperature, as it produced plots of the recorded temperature against the actual interface temperature for different thermocouple distances from the interface. As shortening was recorded with time, when the coefficient of friction was estimated, then interface temperature could be predicted.
Figure 2 shows the relationship between the coefficient of friction and normal stress or interface temperature for various rubbing velocities for the titanium alloy Ti6Al4V. The alloy studied showed sensitivity to rubbing velocity in the range 178 - 480 mm/s. This can be attributed to stick-slip behaviour, as the analytical model shown later suggests. Increasing sliding speed has a direct beneficial effect on thermal softening and simultaneously reduces the time available for surface oxidation. These lead to higher junction growth and larger true area of contact, causing the coefficient of friction to increase slightly as witnessed in the experiments.
To verify the applicability of the experimental procedure followed, intermediate values of the friction coefficient, where a large normal load was applied, were compared to the predicted values of the coefficient. A single test was specifically performed for high temperatures (approximately 800°C). The specimens exhibited noticeable extrusion and the rubbing interface became red. During these experiments, it was verified that the results obtained from the experiments for individual temperatures correlated with realistic situations, where temperatures increase from room temperature to high values during rubbing of materials. The values of the coefficient of friction for intermediate temperatures produced were within 10% of the values expected by the curves fitted to the experimental data. During these experiments plasticity was not observed, therefore, the relation between temperature and stress was linear, as is expected by theory [8].

Results obtained in the frictional behaviour experiments are similar to experimental values reported in literature. In particular [9] the dynamic coefficient of friction of Ti 6Al 4V is reported to be 0.4 and 0.31 in different experimental arrangements. This is not in disagreement with the average room temperature value of 0.43 recorded here. Fluctuations in frictional force were recorded in the experiments, which indicate that stick-slip behaviour is present.

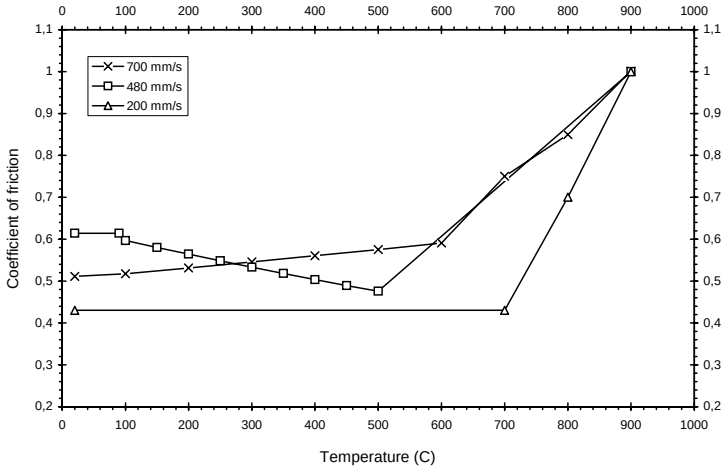

Figure 2. Frictional behaviour of Ti6Al4V

3. LINEAR FRICTION WELDING MODELLING

The characterised frictional behaviour of Ti6Al4V was used to model numerically the process of linear friction welding [10], [11]. Friction is used by the linear friction welding process as a means to clear the rubbing interface of oxides and anomalies, while at the same time generating enough heat for the material at the heat affected zone to reach incipient yield conditions. Due to high temperatures reached, which are below melting temperatures, the interface deforms plastically and allows material to be extruded from the sides of the rubbing interface and finally the two objects are joined together once rest is reached.

The numerical modelling of the welding process had a number of features. The first was thermal-mechanical coupling, as the process is separated into a mechanical and a thermal problem to be solved in parallel during every time step in the analysis. Work done due to friction and plasticity in the mechanical side of the analysis affects the temperature field. Following data transfer from the mechanical analysis, the updated temperatures are taken into account to calculate strains and stresses. This sequential process takes place for every step in the analysis. Another feature of the analysis is material non-linearity, as material properties affect considerably the accuracy of the predictions, where temperature dependent material properties were used to accurately represent the process including the use of viscoplastic constitutive laws for the case of Ti6Al4V. A third feature of the process modelling were the complex thermal boundary conditions, of heat conduction from the rubbing interface to the bulk of the specimens, convection losses to the surrounding air, radiation losses due to the high temperatures reached (of the order of 1000°C) and friction flux as a result of movement between the two specimens. Complex mechanical boundary conditions complicated further the analysis as there was variation with time of both the surface contact area and the frictional parameters, with the friction coefficient changing with temperature as experiments have shown. The surface contact area changes with time due to the sinusoidal movement of the specimens, as will be described later.

Numerical simulations were performed using ELFEN, a proprietary finite element software programme developed by Rockfield Ltd.

The process model of linear friction welding of similar metals can be reduced to half of the original model size, by defining one of the two specimens as rigid, leaving the other object as deformable body. Although frictional heat is generated between deformable and rigid surfaces, temperature rises are effected only on the deformable body, thus reducing the processing time respectively. A total of 764 isoparametric plane stress triangular elements were employed to discretise the two blocks. The top object was set as deformable, while the one at the bottom was set as rigid in an effort to reduce the problem and shorten the analysis time.

The bottom object was constrained in the x and y directions along the bottom face of it. The nodes at the top face of the top block were coupled to move together in both degrees of freedom, as these were the nodes where the oscillatory movement and the friction pressure was applied on. The constraint for the thermal model was to set an initial temperature of 20°C for both objects. The mechanical loads applied were the normal pressure on the top face of the top block, and a prescribed displacement at the corner node of the same face. The displacement changed with time to a sinusoidal function at the required frequency of oscillation. Loading for the thermal analysis included convection and radiation losses.

Non-linear mechanical and thermal material properties were used, whose values depend on temperature. The power law viscoplastic option was employed to represent the material flow rule. The viscoplastic flow rate can be associated to stress conditions in the finite element formulation through the equation:

$$\dot{\tilde{\varepsilon}}^{vp} = \gamma \left[\frac{\tilde{\sigma} - \tilde{\sigma}_y}{\tilde{\sigma}_y} \right]^N \tag{5}$$

From experimental data [12] at the temperatures and strain rates most likely to be encountered in linear friction welding of Ti6Al4V the fluidity parameter γ is set to 2.75E-4 and the exponent N to 4. Contact between the two sliding surfaces was modelled with a series of contact sets, commonly known as slidelines. As the surfaces were in sliding contact, the friction law of Coulomb was used.

Frictional work is generated only when parts of the contact surfaces are in contact. To define the mechanical behaviour of the slidelines a number of associated data are necessary, such as the friction coefficient, taken form the experiments, and parameters for the numerical simulation of deformable bodies.

In order to verify the accuracy of the finite element model developed, two parameters require to be identified:

- the temperature at a known position
- the shear stress conditions

The temperature was recorded using a chromel-alumel thermocouple embedded in a blind hole in the stationary specimen at a predetermined depth.

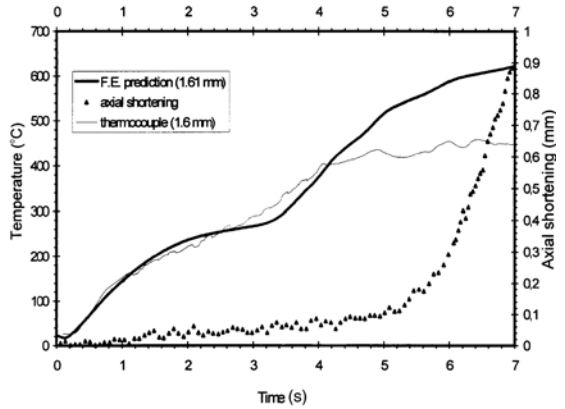

Figure 3. Comparison between experimental data and temperature prediction of the finite element model

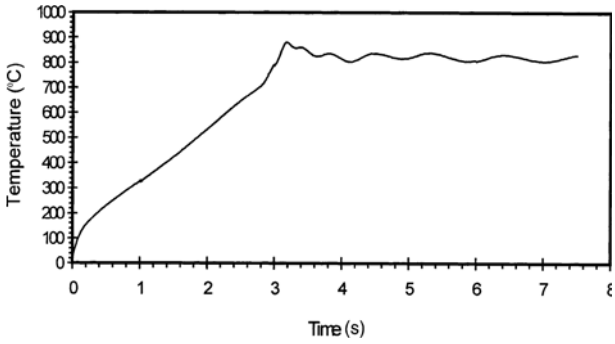

Figure 4. Finite element analysis temperature prediction at rubbing interface

As can be seen (see Fig.3) the temperature prediction of the finite element model closely agrees with the one recorded up to 4 seconds into the process, where they start to deviate. The recorded temperature in the experiment does reach a plateau, before declining. The reason for this lies in the complex metalworking conditions present at the rubbing interface. During the first seconds of the process material is removed from the interface due to wear, and frictional heat raises the temperature at the interface. As material yields locally, either it is extruded from the sides of the specimen, or moves into the hole where the thermocouple is situated. This causes the thermocouple to move away from the interface, where it registers lower temperatures at an unknown distance from the rubbing interface if not damaged.

The finite element model prediction for a node in the middle of the rubbing interface (see Figure 4) predicts that the temperature will not rise above 900°C, and that it will remain steady around that temperature. Although data from thermocouples corroborate the fact that temperatures at the interface should not have exceeded the beta transus temperature of 995°C, metallurgical observations indicated the opposite as acicular alpha was identified in the weld interface. An explanation for this could be that thermocouple measurements can give underestimates of the actual conditions due to the limited control over the thermal inertia, the response time and the positioning of the junction in the specimen.

The finite element model predicted a shear force of 1500 N at 5 seconds into the process, while at the same time the average experimental value was 1425 N, a difference of 5 %.

The finite element model studied the initial stages of linear friction welding of Ti6Al4V and the temperatures predicted by the finite element model were in reasonable agreement with the ones recorded in the experiments by thermocouples close to the rubbing interface. This agreement indicates the consistency between theory and experiment.

4. ANALYTICAL CONTACT MODEL

The irreversible phenomenon of friction originates from the formation and fracture of junctions at the microscopic level formed between the rubbing surfaces, with different regimes relative to sliding velocity. In particular the stick slip regime is associated with cooperative rupture of bonds.
The microscopic model that attempts to relate to macroscopic surfaces motion was reported in literature [13]. Two rigid surfaces are connected by junctions that spontaneously break and form upon contact. The junctions are assumed to behave as elastic springs with a force constant κ and a rest length $l^{(0)}$. A spring of constant K is exerting the necessary force to move the top surface at a constant velocity V. The equation of motion of the driven surface is

$$M\ddot{X} + \eta\dot{X} + F_b + K(x - Vt) = 0 \tag{6}$$

where the force due to the interaction between the junctions and the driven surface is F_b, n being the damping coefficient and q_i being the state of the junction (with q_i=1 for the formed junction and q_i=0 for the breached junction)

$$F_b = \sum_{i=1}^{N} q_i f_i^{(x)} \tag{7}$$

The elastic force f_i from the junction formed is given by Hooke's law, with l being the length of the junction,

$$f_i = \kappa\left[l_i - l^{(0)}\right] \tag{8}$$

The top surface is continuously forming junctions that hinder sliding and extend at the same time. At the same time it is breaking junctions with the bottom stationary surface, similar to spring detachment that assists sliding.
The model junctions extend and contract as the two surfaces slide on each other, with the dynamics of this being represented by velocity

$$\dot{x}_i = q_i\dot{X} - \lambda(1 - q_i)x_i \tag{9}$$

where the junctions extend and compress is considered to be equal to the relative velocity that the two surfaces have. The relaxation constant λ characterizes the approach of a junction to its equilibrium length. This action is different for each junction, as is the length of the junction and the resulting elastic forces are different for each individual junction.
The state of the individual junction q_i can be described in time in terms of the existing number of junctions, the number of junctions formed and the junctions fractured

$$q_i(t + \Delta t) = q_i(t) - q_i(t)\theta\left(\xi_i - \Delta t k_{off}\right) + \left[1 - q_i(t)\right]\theta\left(\xi_i - \Delta t k_{on}\right) \tag{10}$$

where Δt is a time step, ξ_i is a random variable from the interval (0,1) and θ(z) is the Heaviside step function for the description of the stochastic creation and fracture of a junction that occurs for $\xi_i < \Delta t\, k_{off(on)}$. The rate of creation and fracture of junctions is k_{on} and k_{off} respectively.
The junction fracture can be regarded as a thermally assisted escape from a state over an activation barrier $\Delta E(l_i)$, which is dependent on the length of the junction spring and decreases as the elastic energy increases with increasing junction length. Junctions can be of two types: weak junctions where the junction energy is slightly larger than k_BT, with k_B being the Boltzmann constant , and strong junctions, where the energy is much larger than k_BT. In the case of a weak junction the time-dependence fracture rate is

$$k_{off}(l_i) = k_0 \exp\left(\beta f_i \Delta x\right) \tag{11}$$

where $\beta = 1/k_B T$ and Δx being the difference between the maximum and the minimum of the reaction potential. As can be seen, a steady increase in the attracting force produces a small constant bias which reduces the potential barrier. In the case of a strong junction

$$k_{off}(l_i) = k_0\left(1 - f_i/f_c\right)^{1/2} \exp\left\{-\beta\left[U_0\left(1 - f_i/f_c\right)^{3/2} - U_0\right]\right\} \tag{12}$$

Where k_0 is the spontaneous rate of junction fracture when there is no external force present, U_0 the depth of the potential, f_c the critical force at which the potential barrier disappears and is released in the absence of thermal fluctuations.This equation assumes that at a high potential barrier a junction fractures preferentially when the junction is close to slipping.
The junction creation, or reattachment, is characterized by the rate k_{on}, for which is assumed for simplicity that it is not affected by the junction length, but depends on the age of the contact τ. This age τ is the time that the free end of the junction is exposed to the moving interface. The rate of junction creation is dependent on the time difference between the age of the junction τ_0 and the present time $\tau - \tau_0$:

$$k_{on} = k_{on}^0 g\left[\left(\tau - \tau_0\right)/\Delta\tau\right] \tag{13}$$

with k_{on}^0 being the rate of junction creation for a stationary contact, g being a modified stepwise function (where g=0 for junction age $\tau \ll \tau_0$, g=1 for $\tau > \tau_0$). Contact time τ is inversely proportional to sliding velocity, with the contact being related to the typical length scale of the contact α by the equation

$$\tau = \alpha / \dot{X} \tag{14}$$

The characteristic time scale τ_0 , necessary for junction creation, is used to define a critical velocity,

$$V_0 = \alpha / \tau_0 \tag{15}$$

above which junctions cannot be formed. This is necessary in order to accurately represent stick slip conditions.
Applying the model to a large number of junctions (N>300), where the measurable frictional forces are proportional to N, a clear picture emerges of three different frictional behaviour regimes.

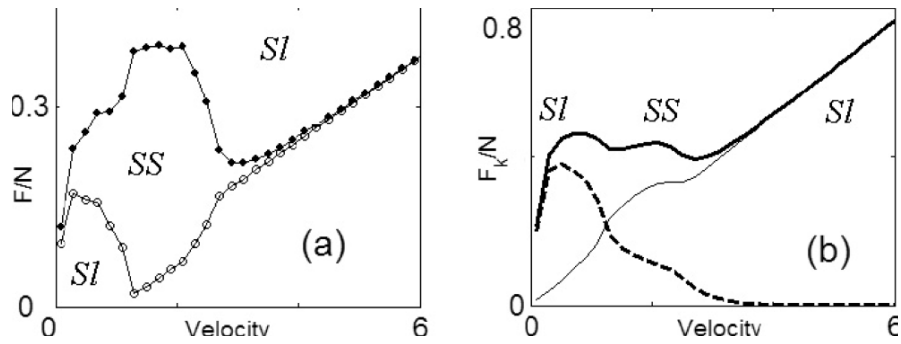

Figure 5 Velocity dependence of time-averaged frictional forces in the case of weak bonds. (a) Maximal (closed circles)and minimal (open circles) spring forces calculated within the microscopic model for weak bonds. (b) The net kinetic friction (bold line), rupture (dashed line), and viscous (thin line) components of the friction force. [*Sl* and *SS* indicate sliding and stick-slip regions correspondingly.] from [12]

There are two sliding regimes with a stick slip region between them. These frictional behaviour regimes can be recognised (
Figure 5) where the time averaged maximal and minimal values of the spring forces are related to sliding velocity through the equation :

$$F = K(X - Vt) \tag{16}$$

The maximal and minimal values of the spring forces coincide in the sliding regime, but differ in the stick slip regime, clearly demonstrating this stick slip behaviour. (see
Figure 5a). This dynamical behaviour has been observed both in the macroscopic, as the above described experiments show, and in the microscopic scale.
The three frictional behaviour regimes exhibit different behaviour, with different mechanisms being responsible for the frictional behaviour observed. The low sliding velocity regime represents a state where thermal bond dissociation determines junction fracture rather that shear induced stress. This regime behaviour correlates with the observation that the value of static friction depends on the time scale. This region is consistent with atomic scale stick slip motion of individual junctions. The low sliding velocity frictional regime, that is characterised by

energy dissipation, is dependent on the fracture and the subsequent relaxation of junctions, rather than on viscous dissipation, as fig. 5B shows.

The stick slip motion region, at an intermediate sliding velocity $V \approx V_c$, the processes of spontaneous and shear induced bond dissociation compete and produce an erratic stick slip motion. The stick slip region has a more regular behaviour as velocity increases $V_0 > V >> V_c$. Junction fracture is controlled by the effect of shear stress on the activation barrier. At this time the fraction of intact junctions decreases with a similar decrease of the fracture contribution to the energy dissipation. The net kinetic friction is relatively insensitive on the sliding velocity in this regime as the effect of the diminishing fractures contribution is counterbalanced by the viscous component of the energy dissipation. The system shows a cooperative behaviour where as the number of breaking bonds increases, the force on the remaining bonds increases and bond rupture synchronises producing a more consistent stick slip behaviour. There is a correlation between macroscopic frictional properties and a collective behaviour of microscopic bonds [14].

The high sliding velocity region shows a transition from stick slip behaviour to smooth sliding. Bond formation becomes impossible due to the short contact time, $\tau < \tau_0$. Frictional force in this regime is completely determined by viscous dissipation

$$F = \eta V \tag{17}$$

5. CONCLUSIONS

The frictional behaviour experiments with dry sliding demonstrated a dependence on interface temperature as well as on rubbing velocity. Although this behaviour is not predicted by the original theories of macroscopic friction, the rubbing velocity dependence of friction coefficient can be explained by an analytical model where two plates are interconnected at the sliding interface with junctions, that continuously form and rupture during sliding. This model demonstrated qualitatively a dependence of frictional behaviour on sliding speed, with stick slip phenomena being responsible for this. It is proposed that the dependence on temperature can be attributed to similar mechanisms of junction formation and fracture and could be explored by its incorporation in the analytical contact model.

Recent studies [15], [16] have shown a promising trend for the modelling of large-scale engineering processes where complex micromechanical phenomena play an important role. It is proposed that the micromechanical models described in the previous section are utilised in order to derive parametrisation at the micro-scale which will enable the accurate modelling of friction welding processes at the macro-scale.

REFERENCES

[1] Amontons, G. (1699), “De la resistance cause dans les machines”, Mem.Del’Academie Royale, A, pp.275-282

[2] Bowden, F.P., Tabor, D. (1950), *Friction and lubrication of solids*, Oxford University Press, England.

[3] Haile, J.M. (1997), *Molecular dynamics simulation: Elementary methods*, John Wiley & Sons, USA.

[4] Greenwood, J.A., Williams, J.B. (1966), “Contact of nominally flat surfaces”, Proc.R.Soc.London, A 295 pp. 300.

[5] Tomlinson, G.A. (1929), “A molecular theory of friction”, Philos Mag., vol.7, no.7, pp.905-939.

[6] Singer. I.L., Pollack, H.M. (1992), *Fundamentals of friction: macroscopic and microscopic processes*, Kluwer, Dordrecht.

[7] Vairis, A. (1997), “Investigation of frictional behaviour of various materials under sliding conditions”, Eur. J. Mech. A/Solids, vol.16, no.6, pp. 929-945.

[8]Rabinowicz, E. (1995), *Friction and wear of materials*, John Wiley &Sons, USA.

[9] ASM Handbook, (1992), *Friction, lubrication and wear technology*, ASM, USA.

[10] Vairis, A., Frost , M. (2000), “Modelling the linear friction welding of titanium blocks”, Mater.Sci.Eng., A292, pp.8-17.

[11] Vairis, A. (1997), *High frequency linear friction welding*, PhD thesis, University of Bristol, England

[12] Chaudhury, P., Zhao, D. (1992), *Atlas of formability : Ti6Al4V ELI*, National Center for Excellence in Metalworking Technology, Johnstown, USA.

[13] Filippov, A.E., Klafter, J., Urbakh, M. (2004), “Friction through dynamical formation and rupture of molecular bonds”, Phys. Rev. Lett., vol.92, 135503.

[14] Budakian, R., Putterman, S.J. (2000), “Correlation between Charge Transfer and Stick-Slip Friction at a Metal-Insulator Interface”, Phys.Rev. Lett., vol.85, no.5, 1000.

[15] Christakis, N. Patel, M.K., Cross, M., Baxter, J., Abou-Chakra, H., Tuzun, U. (2002), “Prediction of segregation of granular material with the aid of PHYSICA, a 3D unstructured, finite volume modeling framework”, Int.J.Numer.Meth.Fluids, vol.40, pp.281-291

[16] Chapelle, P., Christakis, N., Wang, J., Strusevich, N., Patel, M.K., Cross, M., Abou-Chakra, H., Baxter, J., Tuzun, U. (2005), “Application of simulation technologies in the analysis of granular material behaviour during

transport and storage", Proc.I.Mech.E., E : Journal of Process Mechanical Engineering, vol.219, no.1, pp.43-52